ELSEVIER

Thermochimica Acta 379 (2001) 163–175

thermochimica acta

www.elsevier.com/locate/tca

The application of CRTA and linear heating thermoanalytical techniques to the study of supported cobalt oxide methane combustion catalysts

M.J. Tiernan[a,*], E.A. Fesenko[b], P.A. Barnes[b], G.M.B. Parkes[b], M. Ronane[a]

[a]*School of Chemical Sciences, Dublin City University, Dublin 9, Ireland*

[b]*Centre for Applied Catalysis, Materials Research Division, University of Huddersfield, Queensgate, Huddersfield HD1 3DH, UK*

Abstract

Two combined thermal analysis-mass spectrometry techniques have been used to ascertain the effects of various support materials on the preparation and subsequent combustion activity of supported cobalt oxide catalysts. Both techniques used small sample masses in order to minimise temperature and pressure gradients throughout the sample during reaction as the sample temperature was increased at a linear heating rate. Temperature-programmed reduction (TPR) techniques employed not only reveal reduction, but also distinguish it from the adsorption (or evolution) of the H_2 and the loss of absorbed water. The thermally induced decomposition of supported and unsupported cobalt nitrate hexahydrate was studied using a solid insertion probe mass spectrometer (SIP-MS) system operating under high vacuum. The support material was found to affect the decomposition process significantly. In particular, the decomposition of cobalt nitrate dispersed on γ-Al_2O_3 occurred via a markedly altered process in comparison with the unsupported nitrate. The ZrO_2 and CeO_2 supports both exhibited less pronounced effects on the decomposition process. After calcination of dispersed cobalt nitrate species, methane combustion activity was found to be much lower for alumina-supported samples relative to the other supports used. A combined temperature-programmed reduction–mass spectrometry (TPR–MS) technique was used to elucidate a correlation between catalyst activity and reducibility. The reduction of a Co_3O_4/CeO_2 catalyst was also studied under constant rate thermal analysis (CRTA) conditions.

Keywords: Combustion catalysts; Solid insertion probe-mass spectrometry (SIP-MS); Cobalt oxides; Temperature-programmed reduction (TPR); Constant rate thermal analysis (CRTA)

1. Introduction

Catalytic combustion of hydrocarbons is of widespread importance for applications such as gas turbines, boilers, domestic heaters, automotive exhaust catalysts and VOC removal from industrial effluents. Compared to thermal combustion processes, the presence of a catalyst gives better control of oxidation over wider fuel:air ratios, lowers the operating temperatures, which results in reduced nitrogen oxide emissions and can also provide improved energy recovery giving a more efficient use of fuel [1]. The most widely used catalysts are noble metals (e.g. Pt, Pd), transition metal oxides (e.g. CuO, Co_3O_4) and mixed oxide systems (e.g. perovskite oxides, $CuAl_2O_4$) [2]. The intrinsic activity of noble metals is known to be higher than that of simple metal oxides for hydrocarbon oxidation so their use as combustion catalysts is normally

* Corresponding author. Tel.: +353-1-7005134; fax: +353-1-7005503.
E-mail address: michael.tiernan@dcu.ie (M.J. Tiernan).

0040-6031/01/$ – see front matter
PII: S0040-6031(01)00614-1

favoured [3]. For example, in automobile catalytic converters, a mixture of noble metals (Pt, Pd and Rh) stabilised on an Al_2O_3 support is used to clean-up exhaust emissions with Pt and Pd being the main active ingredients for the combustion of hydrocarbons to CO_2 and H_2O. However, the depletion of Pt and Pd reserves and the associated rise in precious metal prices means that the discovery of cheaper, more abundant alternatives for catalytic combustion applications is an important aim in the scientific community.

The current paper reports studies of the potential use of supported and unsupported cobalt oxides for the combustion of methane. Particular emphasis is placed on the role played by various thermal analysis methods in the elucidation of factors which affect catalyst performance.

Since the concentration of methane in the atmosphere is rising, its elimination via conversion to carbon dioxide, which has a lesser greenhouse effect, is becoming increasingly important [4]. Methane is the most inert hydrocarbon and hence, the most difficult to destroy by complete combustion at low-temperatures. World-wide efforts to find less expensive options to noble metal catalysts for this process are being made [4–6]. Early studies on the use of simple metal oxide systems reported Co_3O_4 as being the most active catalyst of a variety of base metal oxides tested for the oxidation of paraffins including methane [3,7,8]. More recently, the potential of cobalt as a viable alternative to, or additive in, noble metal combustion catalysts has been highlighted [9–12]. Deactivation problems exist due to sintering of the active Co_3O_4 phase and reaction with alumina supports forming inactive mixed oxides. However, despite such problems with existing formulations, research into the use of Co_3O_4 may provide a greater understanding of the origins of low-temperature combustion activity. This is particularly important in terms of automotive exhaust applications in the drive to develop new catalytic technologies to reduce 'cold-start' emissions problems [10]. Such difficulties relate to the fact that a large proportion of the uncontrolled emissions from cars equipped with catalysts stem from the first few minutes of driving when the catalyst has not yet reached a temperature at which it can operate effectively. Hence, there is a need for the development of catalytic formulations which start to covert pollutants at lower temperatures thereby reducing unwanted automotive emissions.

It is known that the support material employed for the dispersion of noble metal or metal oxide active species can have a significant effect on the methane combustion activity of the dispersed species [7,13]. On evaluation of a wide variety of supported and unsupported oxides, Anderson et al. [7] reported that Co_3O_4 was the most active for the combustion of methane. However, when impregnated on an alumina support, performance was found to be lower than a range of other supported oxides. This deactivation was explained in terms of a possible formation of a $CoAl_2O_4$ spinel structure. Strong interaction of dispersed Co species with alumina support materials has been widely reported to cause a decrease in the activity of supported Co_3O_4 combustion catalysts [10,14]. In the present study, a variety of different materials (alumina, ceria and zirconia) have been employed as supports for cobalt oxide catalysts in an attempt to determine the importance of the support on catalytic activity for methane combustion.

Solid insertion probe-mass spectrometry (SIP-MS) was used to study the decomposition of catalyst precursor species on the various support materials. The advantages of using this technique for the study of thermally induced decompositions have been previously described [15]. In brief, a combination of small sample mass, which reduces temperature gradients, and high vacuum (10^{-5} Pa), which minimises diffusion problems and the possibility of back reaction between the solid product and evolved gases, makes the SIP-MS highly suited for the study of calcination or decomposition processes. This is the first example of an application of the technique in the study of catalyst preparation.

A temperature-programmed reduction–mass spectrometer (TPR–MS) technique was employed for the characterisation of the oxide catalysts formed following calcination of the precursor in air with the aim of defining a correlation between redox properties and catalytic activity. The use of a mass spectrometer as the detector for TPR studies allows for direct simultaneous monitoring of H_2 uptake and H_2O evolution, providing a greater insight into the reduction process relative to the more commonly used thermal conductivity detectors which monitor only H_2 uptake as a function of temperature [16] or the use of a

hygrometer to monitor H_2O evolution, but which provides no information on H_2 uptake [17].

A major advantage of using a mass spectrometer is, therefore, the ability to reveal the evolution or adsorption of H_2 (i.e., where no H_2O is evolved) and the drying of the samples (i.e., where no H_2 is consumed) and to clearly distinguish these processes from reduction, where there is a simultaneous decrease in hydrogen and increase in water vapour.

In addition to the use of conventional linear heating rate TPR, the reduction of supported cobalt oxide was also studied under constant rate thermal analysis (CRTA) conditions. In constant rate–temperature-programmed reduction (CR–TPR), the rate of reduction is regulated to maintain a constant rate of reactant consumption or product formation by controlling the sample temperature appropriately. This approach is capable of producing higher resolution of overlapping events, allowing easier quantification of reduction events while the shape of the temperature profile obtained can provide a limited insight into the reduction mechanism [17].

2. Experimental

2.1. Catalyst preparation

Unsupported cobalt oxide samples (CoO and Co_3O_4) were supplied by Aldrich. Supported cobalt oxide samples were prepared by a wet impregnation technique using aqueous solutions of $Co(NO_3)_2{\cdot}6H_2O$ (BDH, laboratory reagent, >97% purity). The powdered support materials used were γ-Al_2O_3 (supplied by Condea), ZrO_2 (Aldrich, 99%) and CeO_2 (Sigma, 99.9%). Impregnation was achieved by dissolving an appropriate amount of the nitrate salt in 9 cm^3 of H_2O followed by addition of 3 g of the support material. After mixing for 90 min, excess water was removed using a cold trap (liquid N_2–toluene) rotary evaporator. Samples were then dried at 45°C overnight and at 110°C for 8 h. Calcination of supported nitrate samples to produce cobalt oxide(s) was achieved in a static air muffle furnace at either 400 or 600°C for 1 h. The level of cobalt in the supported samples prepared was nominally 5 or 15 wt.% based on the amount of the nitrate employed in the impregnation step. γ-Al_2O_3 supported Pt and Pd samples, containing a nominal noble metal loading of 0.5 wt.%, were prepared by impregnation of the support with solutions of $H_2PtCl_6{\cdot}6H_2O$ and $PdCl_2$, respectively. After drying, calcination was performed by heating at 630°C in static air for 15 min.

The decomposition process of unsupported cobalt nitrate hexahydrate was studied by simultaneous TG-DSC (STA) using a Stanton Redcroft STA 625 instrument. The sample (10 mg) was placed in an aluminium crucible and heated at 10°C min^{-1} from room temperature to 600°C in an air atmosphere.

The decomposition of supported and unsupported cobalt nitrate samples was also studied using the SIP-MS system, which has been described in detail previously [15]. The SIP consists of a cylindrical microfurnace (12 mm × 5 mm) positioned at the end of a water-cooled stainless steel rod which can be located, via airlock valves, directly into the source chamber of a VG Micromass 7070HS mass spectrometer. Important instrumental features include sample temperature measurement via a thermocouple (type K, chrome–alumel) located at the base of the sample holder to place it in virtually direct contact with the sample itself. The SIP can be heated to 1000°C and sample masses are typically <10 mg. Linear heating rate experiments were performed using 10 ± 0.3 mg of sample at various heating rates of between 1 and 10°C min^{-1}. The mass spectrometer is a sensitive and stable double-focusing magnetic sector instrument which was operated in "peak select" mode with a multiple ion detector (MID) unit operated in field switching mode to allow direct monitoring of five ions: $m/z = 18$ (H_2O); $m/z = 30$ (NO); $m/z = 32$ (O_2); $m/z = 44$ (N_2O or CO_2); and $m/z = 46$ (NO_2). Ions were monitored consecutively for a period of 500 ms each as the SIP temperature was increased from room temperature to 600°C. The response for $m/z = 30$ was used as a measure of the evolution of NO_x species since this m/z value may be associated with NO, NO_2 or N_2O.

2.2. Catalyst characterisation

The specific surface areas of catalysts were determined by N_2 adsorption at −196°C according to the BET method using a Micromeritics Gemini instrument. X-ray diffraction (XRD) spectra were obtained using Cu Kα ($\lambda = 1.5418$ Å) radiation in order to allow identification of the crystalline phases present.

TPR–MS experiments were performed on supported and unsupported cobalt oxide samples using a reduction atmosphere of 5% hydrogen in helium at a flow rate of 50 $cm^3\ min^{-1}$. Supported samples were analysed after calcination at 400°C. After passage through the sample bed (30–50 mg) the effluent gas stream passed into the source chamber of the VG Micromass 7070HS mass spectrometer via a jet separator. The MID unit was used to directly monitor the following ions: $m/z = 18$ (H_2O); $m/z = 17$ (H_2O); $m/z = 2$ (H_2); and $m/z = 1$ (H_2) as the sample was heated upto 850°C. Conventional TPR experiments were performed using a linear heating rate of 10°C min^{-1}. CR–TPR was performed using maximum heating and cooling rates of +10 and −10°C min^{-1}, respectively, with the heating rate varied between these limits in order to maintain a constant preselected water evolution rate (i.e. reduction rate) of ca. 7×10^{-3} mg $H_2O\ min^{-1}$. The software and instrumentation used for data acquisition and control in CRTA–MS experiments have been described in detail previously [15].

2.3. Catalytic combustion activity

Catalytic activity for the combustion of methane was monitored as a function of temperature using a continuous flow apparatus. A stoichiometric mixture of methane in air (ratio, 1:10) at a total flow rate of 33 $cm^3\ min^{-1}$ was passed through 0.3 g of the catalyst sample held on a sintered disc in a quartz U-tube. As the sample was heated, unreacted methane was monitored at specific temperatures, within the range 20–600°C, by in situ gas chromatography (Schimadzu GC-14A) using a packed Poropak Q column and a flame ionisation detector. At each furnace temperature, the effluent stream leaving the sample was monitored for at least 15 min until equilibrium was attained. After a first cycle of tests (Run 1) all catalysts were cooled to room temperature in air and re-tested (Run 2). The exact temperatures at which catalytic activity was monitored varied from one sample to another. Typically, activity was monitored at room temperature, 100, 200 and at 50°C intervals from 200 to 600°C. At some temperatures, considerably longer than 15 min was required for equilibrium to be attained.

3. Results and discussion

3.1. Decomposition of catalyst precursors

Fig. 1 illustrates thermoanalytical curves obtained for the unsupported nitrate using simultaneous TG and DSC. The overall weight loss observed corresponds to

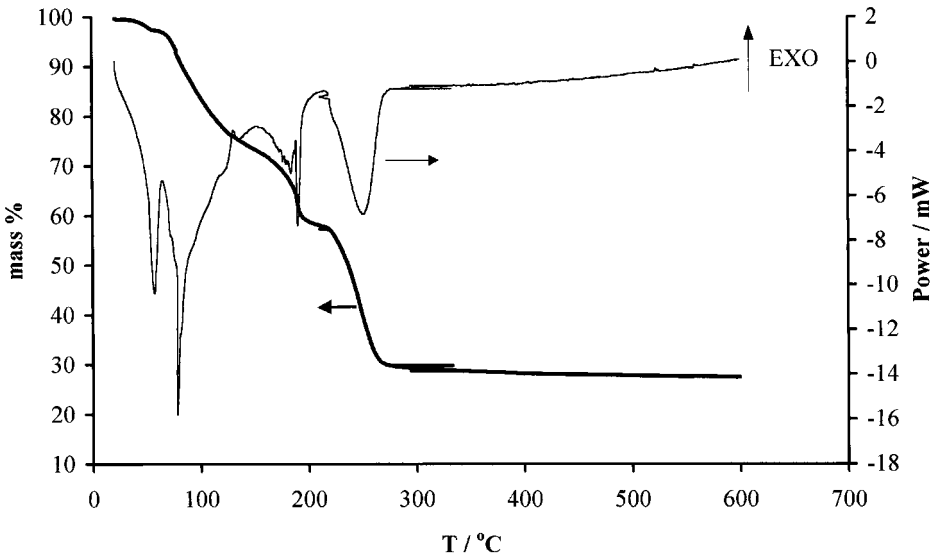

Fig. 1. Simultaneous TG–DSC curves of the decomposition of $Co(NO_3)_2{\cdot}6H_2O$.

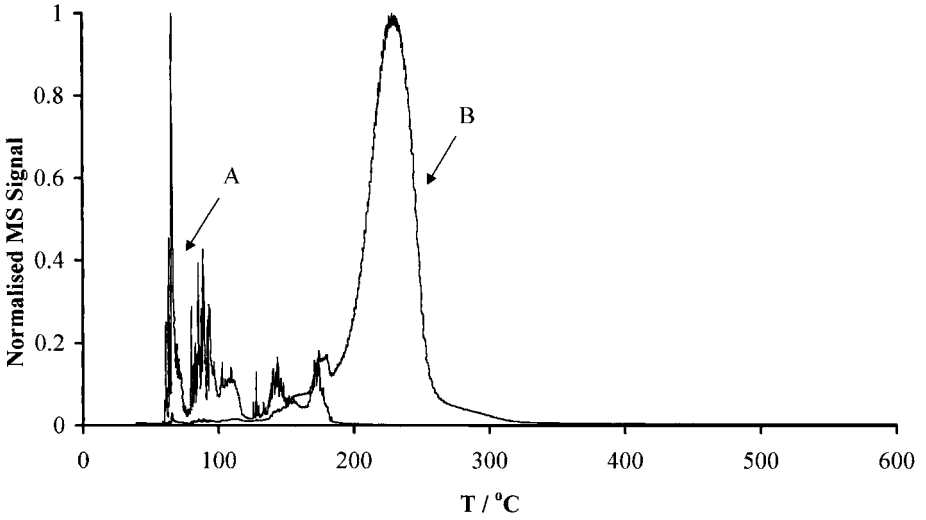

Fig. 2. SIP-MS profile of the decomposition of $Co(NO_3)_2{\cdot}6H_2O$ at a linear heating rate of 6°C min^{-1}, showing the evolution of H_2O (A) and NO_x (B) species as a function of temperature.

conversion to Co_3O_4 as the product of the decomposition. The weight loss below 200°C can be accounted for by loss of water of crystallisation, along with a small amount of adsorbed water. Subsequent decomposition evolving NO_x species and yielding the oxide product occurred in a single endothermic step between ca. 210 and 280°C. In agreement with previous studies [18,19], SIP-MS data showed that water evolution was almost complete prior to the onset of the nitrate decomposition (see Fig. 2). The decomposition of bulk metal nitrates can occur with or without concomitant dehydration [18]. In the case of cobalt nitrate, Cseri et al. [18] reported that loss of water occurred in a preliminary step separate to the main decomposition to the oxide. However, as found in the current study, this H_2O release was not completed prior to the onset of NO_x evolution as shown by TG–DTG–DTA–MS experiments performed using a heating rate of 6°C min^{-1} in flowing N_2 atmosphere [18]. Similarly, Mansour [19] reported that the decomposition proceeded to Co_3O_4 as the final product in flowing air with decomposition completed at 280°C. The nitrate hexahydrate was found to undergo melting at 75°C followed immediately by dehydration to produce cobalt nitrate monohydrate and again nitrate decomposition began prior to completion of the dehydration process [19].

The effect of the support on the nitrate decomposition process was investigated in the current work using SIP-MS to follow the evolution of NO_x species as a function of temperature. Results obtained for the unsupported and supported (5 wt.% Co) samples using a linear heating rate of 6°C min^{-1} are compared in Figs. 2 and 3, respectively. A marked effect of the support on the decomposition profile was observed. For the unsupported sample (Fig. 2), most of the decomposition occurred in a single peak within a temperature range of 150–300°C with a maximum rate of evolution of NO_x species at 230°C. In the case of the zirconia (Fig. 3(A)) and ceria (Fig. 3(B)) supported materials, decomposition occurred over much broader temperature ranges of ca. 150–400°C. The most marked difference between supported and unsupported samples was observed for the alumina-based system with decomposition being split into two separate processes with peak temperatures of 355 and 465°C and completion of decomposition was delayed until 600°C (Fig. 3(C)).

3.2. Catalyst characterisation

Table 1 summarises the BET surface areas measured for supported and unsupported cobalt oxide samples and for the support materials themselves.

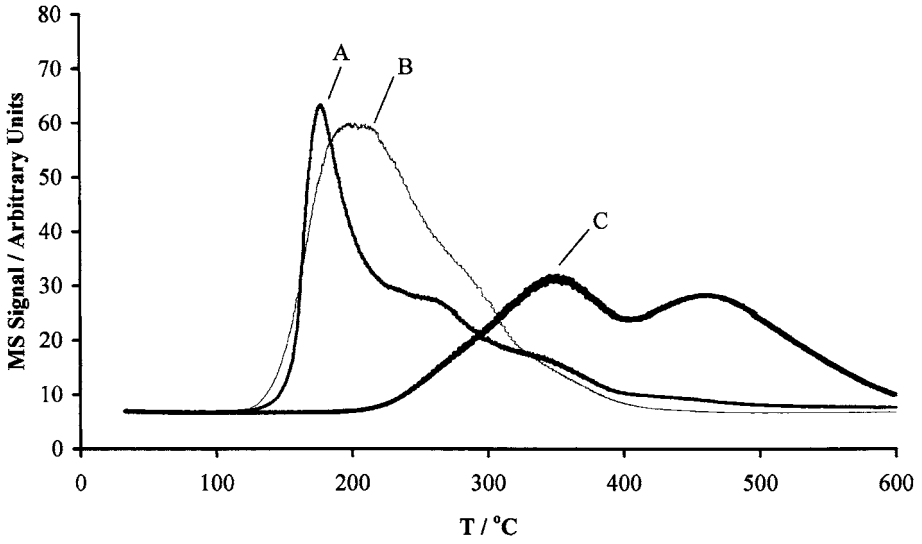

Fig. 3. SIP-MS profile of the decomposition of supported $Co(NO_3)_2{\cdot}6H_2O$ at a linear heating rate of 6°C min^{-1}, showing the evolution of NO_x species ($m/z = 30$) as a function of temperature for various support materials. (A) ZrO_2; (B) CeO_2; (C) Al_2O_3.

Due to the high surface area of the γ-Al_2O_3 support, a higher dispersion of supported Co species will be expected relative to the CeO_2- and ZrO_2-based systems. XRD patterns obtained for samples with 15 wt.% Co showed the presence of Co_3O_4 crystallites on all support materials after calcination at 400°C.

TPR profiles of supported samples are shown in Figs. 4–6 illustrating H_2 uptake ($m/z = 2$) and H_2O evolution ($m/z = 18$) as a function of sample temperature. The relative areas of the H_2 uptake and H_2O evolution peaks could not be compared quantitatively due to the use of a jet separator inlet which, due to mass discrimination effects, resulted in a much smaller proportion of the H_2 (compared to H_2O) content of the product gas entering the source chamber. However, it is apparent from Figs. 4–6 that H_2 uptake and H_2O evolution occurred simultaneously in the reduction peaks observed.

Table 1
BET surface areas of supported and unsupported catalysts

Sample	Co content (mass%)	Surface area ($m^2\ g^{-1}$)
CoO	–	8
Co_3O_4	–	23
ZrO_2	–	5
Co/ZrO_2	5	4
CeO_2	–	33
Co/CeO_2	5	22
Al_2O_3	–	215
Co/Al_2O_3	5	191

For the 15 wt.% Co/ZrO_2 sample (Fig. 4), two overlapping peaks are apparent with maxima at 312 and 357°C. Both peaks can be associated with the reduction of cobalt oxide species as the support showed no reduction peaks within this temperature range. Arnone et al. [11] reported a similar TPR profile for unsupported Co_3O_4 containing two overlapping peaks (maxima at 382 and 470°C) which was explained in terms of initial reduction from the average oxidation state of 2.7+ (Co_3O_4) to 2+ (CoO) followed by subsequent reduction from the 2+ to metallic oxidation state to metallic product. Complete reduction to Co^0 was confirmed by XRD carried out after TPR upto 600°C at 10°C min^{-1} [11]. Meaningful comparison of peak temperatures with those found in the current study is difficult due to variations in experimental conditions [17] and known differences in the reducibility of supported and unsupported metal oxides [20]. The TPR profile obtained for 15 wt.% Co/CeO_2 in the current study (Fig. 5) also shows two overlapping peaks at temperatures of 305 and 352°C which, again, may be attributed to a two-stage reduction of Co_3O_4 to metallic cobalt via CoO. A higher

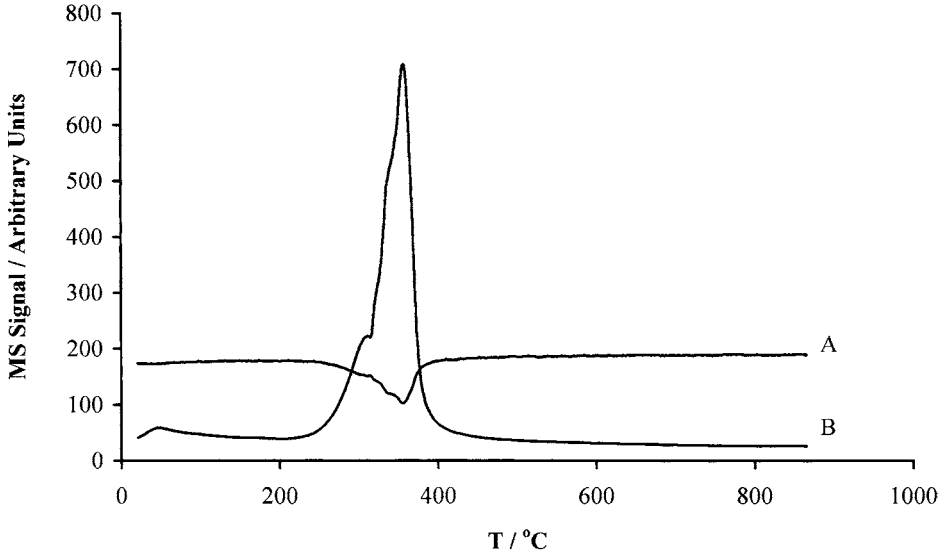

Fig. 4. TPR profile of 15 wt.% Co/ZrO_2 at a linear heating rate of 10°C min^{-1}. Sample size = 42 mg. (A) H_2; (B) H_2O.

temperature reduction peak observed at above 700°C can be attributed to some support reduction, as was confirmed by TPR experiments on the pure support material.

For the 15 wt.% Co/Al_2O_3 sample, a more complicated TPR profile was produced (Fig. 6). The initial H_2O evolution peak below 100°C may be associated with adsorbed water on the high surface area support material as it decreased considerably in size when the sample was dried overnight at 110°C in flowing He. It is known from numerous previous investigations [21–23] that γ-Al_2O_3-supported cobalt oxide catalysts

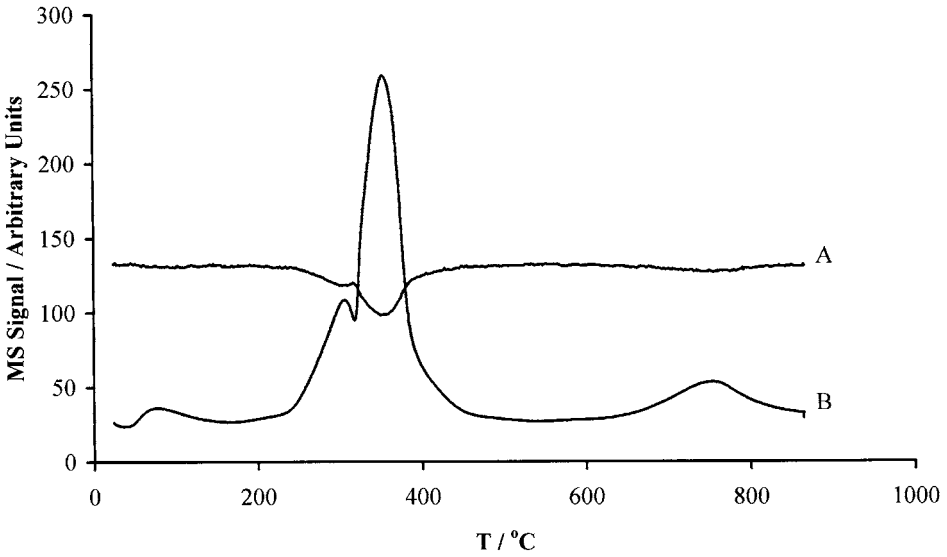

Fig. 5. TPR profile of 15 wt.% Co/CeO_2 at a linear heating rate of 10°C min^{-1}. Sample size = 34 mg. (A) H_2; (B) H_2O.

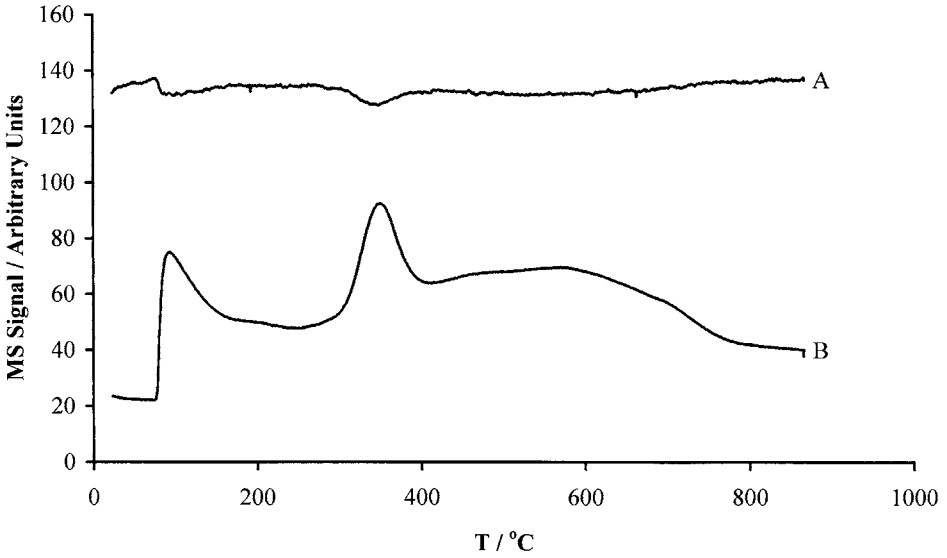

Fig. 6. TPR profile of 15 wt.% Co/Al_2O_3 at a linear heating rate of 10°C min^{-1}. Sample size = 40 mg. (A) H_2; (B) H_2O.

comprise mainly of two types of cobalt-containing phases, namely (i) surface phases of Co bonded to the support which are relatively difficult to reduce and which prevail at lower Co concentrations and on higher surface area supports, and (ii) a more easily reducible Co_3O_4 phase which appears above a Co concentration of ca. 2 wt.%. The former phases include cobalt aluminates such as $CoAl_2O_4$ formed when Co ions occupy tetrahedral positions in the Al_2O_3 lattice during preparation, and overlayer Co^{3+} and Co^{2+} species [21–23]. On this basis, the peak at 350°C in Fig. 6 may be attributed to the reduction of a Co_3O_4 phase while the higher temperature reduction feature (up to >800°C) is most probably associated with the reduction of one or more phases involving strong interaction of dispersed Co species with the support material formed during catalyst preparation. Formation of such phases, which might also explain the retarded thermal decomposition of γ-Al_2O_3-supported cobalt nitrate (see Fig. 3), was difficult to ascertain from the XRD patterns obtained because of the broad nature of support peaks observed and the highly dispersed (and/or X-ray amorphous [22,23]) nature of the species involved.

In linear heating rate TPR profiles, difficulties can exist with the resolution and hence quantification of overlapping reduction events [17,22] with supplementary techniques such as XRD often required to elucidate the steps observed [24]. For example, Arnoldy and Moulign [22] reported that only one reduction peak was observed for bulk Co_3O_4 in a linear heating rate TPR profile with evidence for two-stage reduction coming solely from the fact that the peak was broader than that obtained in the profile for CoO under the same experimental conditions. A less pronounced lack of resolution of overlapping peaks in the current study means that exact quantification of the two events involved in the reduction of Co_3O_4 crystallites supported on ZrO_2 and CeO_2 is difficult to achieve from the linear heating rate profiles obtained (see Figs. 4 and 5).

In an attempt to provide greater resolution and an improved quantitative insight into the reduction process, the reduction of the CeO_2-supported sample was studied under CRTA conditions. Fig. 7 shows a CR–TPR profile obtained for 15 wt.% Co/CeO_2. The temperature trace shows how the sample temperature was continuously altered to maintain, as far as possible, the constant pre-selected rate of reduction. It can be seen that the rate of H_2O production was maintained at an approximately constant level throughout the reduction of cobalt oxide occurring in the temperature range of 200–280°C. As for the linear heating rate profile (Fig. 5), the reduction feature at higher temperatures in Fig. 7 is again attributable to support reduction.

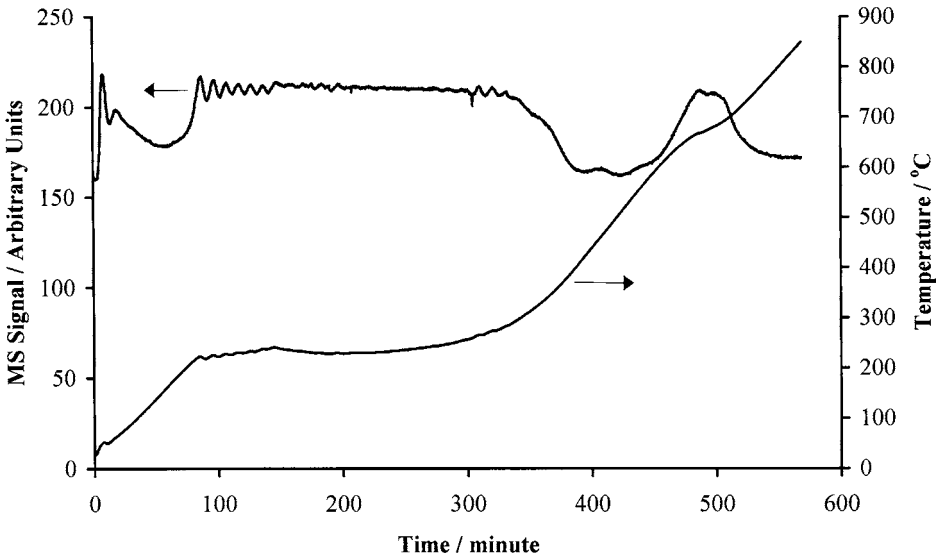

Fig. 7. CR–TPR profile of 15 wt.% Co/CeO_2. Sample size = 33 mg.

Fig. 8 compares the α (extent of reaction) versus temperature (T) profiles for the reduction of cobalt oxides in a 15 wt.% Co/CeO_2 catalyst under linear heating (Fig. 8(A)) and CR–TPR (Fig. 8(B)) conditions. In both cases, the reduction feature associated with the support material is not shown (i.e., $\alpha = 1$ refers to completion of cobalt oxide reduction only). This form of presentation can be valuable for quantitative comparison of the two TPR methods. The profiles obtained under CR–TPR conditions were found to be somewhat dependent on sample preparation and experimental parameters. Under the conditions employed to obtain the profile in Fig. 8(B), it is apparent that reduction proceeds at a lower temperature

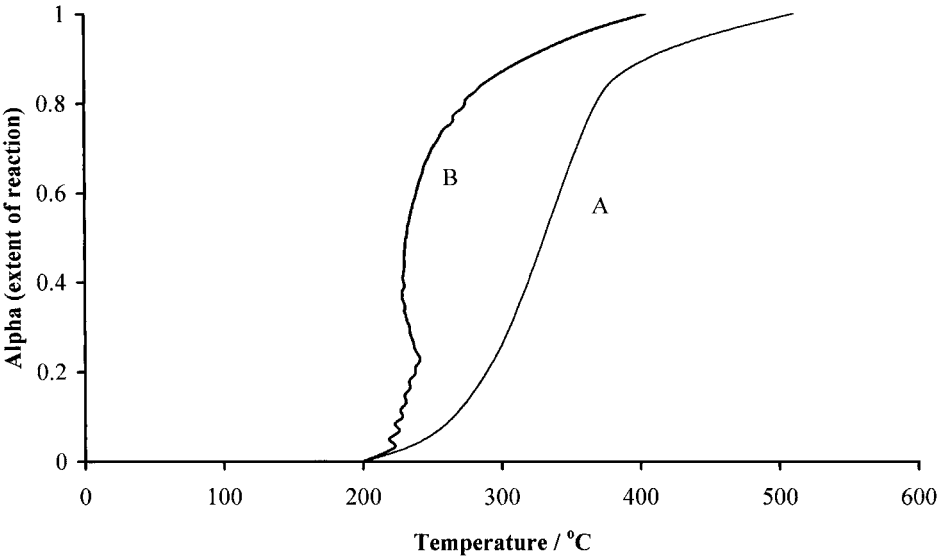

Fig. 8. The α vs. temperature profile for the reduction of 15 wt.% Co/CeO_2 under (A) linear heating and (B) CR–TPR conditions.

in the CR–TPR experiment. This is due to the fact that the target reduction rate was considerably lower than the maximum rate of reduction achieved in the linear heating experiment. No distinct resolution of the two reduction events is apparent in the α versus T curve obtained in the linear heating experiment (Fig. 8(A)). However, under the CR–TPR conditions employed, a change in the nature of the heating regime required to maintain a constant rate of reduction is apparent after $\alpha \cong 0.25$. This indicates that the reduction of Co_3O_4 proceeds in a stepwise manner possibly involving complete conversion to CoO prior to subsequent reduction to metallic Co as follows:

$$Co_3O_4 + H_2 \rightarrow 3CoO + H_2O \quad (\text{step } 1)$$

$$3CoO + 3H_2 \rightarrow 3Co + 3H_2O \quad (\text{step } 2)$$

with step 1 accounting for 25% of the total H_2O production. The unfamiliar shape of the α versus T profile in Fig. 8(B) can be interpreted in terms of the kinetic mechanism of each reduction step and the effect which the mechanism followed has on the heating regime required as follows.

The change in shape of the α versus T profile in Fig. 8(B) after the reduction is ca. 25% complete suggests that the mechanisms of reduction in steps 1 and 2 are different under the experimental conditions employed. The kinetics of solid-state reactions such as gas–solid reductions are generally interpreted in terms of kinetic models categorised as involving either diffusion-controlled, boundary-controlled or nucleation-controlled processes and each of these three classes of mechanism produces a characteristic α versus T curve shape in CRTA experiments [15,25]. In Fig. 8(B), it is seen that below $\alpha = 0.25$, although there is some fluctuation in the detector response, the temperature has effectively to increase continuously to maintain the pre-selected constant rate of H_2O evolution indicating that step 1 (i.e., reduction of Co_3O_4 to CoO) followed a phase boundary-controlled mechanism ('n-order' expression), where nucleation or diffusion are not the rate-controlling factors [15,25]. In contrast, the 'U-shaped' α versus T curve seen at $\alpha > 0.25$, corresponding to subsequent reduction of CoO to Co, is characteristic of a nucleation and/or autocatalytic reduction mechanism [17,20,25]. The limitations of this kinetic interpretation warrant documentation. In particular, differences in the mechanism of reduction of the two steps indicated in Fig. 8(B) may only be representative of the applied conditions since solid-state kinetic parameters can be influenced by the experimental conditions employed. A more in-depth analysis of the effects of experimental conditions and the application of multi-heating rate and/or CRTA 'rate-jump' methods would be needed in order to ascertain more meaningful details regarding the overall kinetic parameters (the reaction model, activation energy and Arrhenius pre-exponential factor) and any variation in these parameters with the extent of reaction [17,26].

3.3. Catalytic activity tests

Preliminary tests, performed under the same conditions as the catalytic tests, but without any catalyst, showed that homogeneous reactions are negligible under the experimental conditions investigated.

The results of catalytic activity tests for unsupported Co_3O_4 and CoO are shown in Fig. 9. Both catalysts gave almost complete conversion of methane (>99%) within 600°C. Co_3O_4 (Fig. 9, catalyst A) was found to be more active than CoO (Fig. 9, catalyst B) with equivalent levels of conversion achieved at lower temperatures on the former phase. In a review of the principles of oxidative catalysis, Sokolovskii [27] noted that the most active metal oxide combustion catalysts, including cobalt oxide, bind oxygen at a fast rate to produce a high concentration of reactive negatively-charged species on the catalyst surface. Finocchio et al. [28] also predicted that the mechanism of hydrocarbon combustion over metal oxides, including Co_3O_4, involved surface nucleophilic lattice oxygen species. Arnone et al. [11] reported a relationship between the catalytic activity of metal oxides in methane combustion and catalyst reducibility with availability of surface lattice oxygen believed to significantly affect catalytic properties. Therefore, increased activity for Co_3O_4 relative to CoO is not unexpected in the light of its increased reducibility at lower temperatures and the higher surface area of the Co_3O_4 sample.

On re-testing the unsupported oxides in Run 2, both showed a loss of activity (see Fig. 9) suggesting that both undergo deactivation under the reaction conditions. This may be attributable to sintering of the active phase (which has been previously reported to occur on heating of Co_3O_4 to 600°C [19]) resulting in

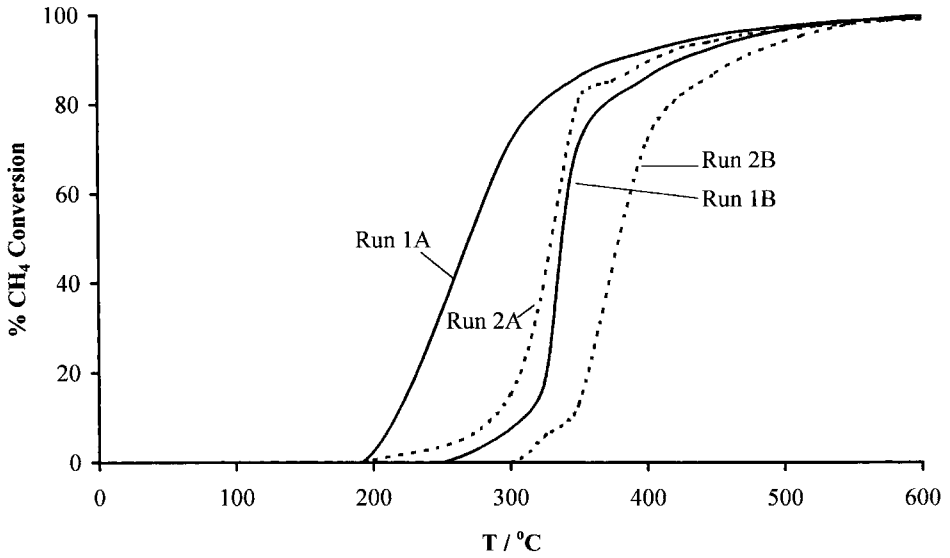

Fig. 9. CH_4 conversion as a function of temperature for bulk Co_3O_4 (Runs 1A and 2A) and CoO (Runs 1B and 2B).

a lower surface area available for adsorption or reaction of gaseous components [10]. The BET surface areas of the CoO and Co_3O_4 samples decreased by 63% to 3 $m^2\ g^{-1}$ and by 43% to 13 $m^2\ g^{-1}$, respectively, upon testing in the reaction mixture for Runs 1 and 2. In the case of Co_3O_4, deactivation may also have been related to conversion to less active CoO phase at temperatures above 450°C [11]. The presence of CoO, as well as Co_3O_4, was indicated in the XRD pattern of the Co_3O_4 sample obtained after testing in Runs 1 and 2.

Table 2 reports the temperatures (T_{50} values) at which methane conversion exceeded 50% over the various supported and unsupported samples tested. T_{50} values for Al_2O_3-supported Pt and Pd catalysts are also shown for comparison purposes. This temperature is usually denoted the 'light-off' temperature and is off particular importance in relation to the 'cold-start' emissions problem in automotive exhausts discussed above [10].

The most active supported catalyst tested was 0.5 wt.% Pd/Al_2O_3 which achieved 50% conversion at a temperature of 330°C (see Table 2). Higher activity for Pd relative to Pt for the combustion of methane has been related to the different abilities of the two metals to adsorb oxygen [29–31]. It should be noted that the Pd surface was not reduced prior to testing and as such the activity measured may not have been optimal. In the current study, both Co/ZrO_2 and Co/CeO_2 samples, which were calcined at 400°C prior to testing, showed higher activity than Pt/Al_2O_3, although it should be noted that the concentration of metal (wt.%) was 10–20 times higher in the case of the cobalt samples tested. A low concentration of noble metal was employed due to expense considerations. Considering the support materials in the absence of cobalt, CeO_2 showed some combustion activity at

Table 2
Temperature of 50% CH_4 conversion for cobalt catalysts

Sample	Metal content (mass%)	Calcination temperature (°C)	T_{50} (°C)	
			Run 1	Run 2
Pt/Al_2O_3	0.5	630	470	475
Pd/Al_2O_3	0.5	630	330	330
Co/Al_2O_3	5	400	>500	>500
Co/ZrO_2	5	400	390	425
Co/Al_2O_3	5	600	>500	>500
Co/ZrO_2	5	600	490	500
Co/CeO_2	5	600	410	495
Co/Al_2O_3	15	400	>500	>500
Co/ZrO_2	15	400	395	420
Co/CeO_2	15	400	340	435
Co_3O_4	–	–	270	330
CoO	–	–	340	380
CeO_2	–	400	540	535

higher temperatures within the range investigated in line with previous observations that it is an active methane combustion catalyst at elevated temperatures [32]. However, T_{50} was considerably lower in the presence of Co, particularly for Run 1 (see Table 2) during which CeO_2 did not contribute to the light-off activity (i.e., conversion at T_{50}) of the supported Co catalysts tested since on its own it showed no combustion activity at or below 400°C. During Run 2, a methane conversion of 5% was achieved over CeO_2 at the light-off temperature of the 15 wt.% Co/CeO_2 sample indicating that the majority of light-off performance for this sample was still related to the presence of the cobalt. In the case of both ZrO_2 and Al_2O_3 supports, no appreciable activity existed below 500°C.

It is known that the use of Al_2O_3 as the support medium can significantly decrease the activity of cobalt-based combustion catalysts [7,21]. From Table 2, it can be seen that ZrO_2 and CeO_2 supported samples were considerably more active that the corresponding Al_2O_3 supported catalyst. This is further illustrated in Fig. 10 which compares results for the conversion of methane as a function of temperature upto 500°C over supported cobalt catalysts containing 15 wt.% Co. The lower activity for the high surface area Al_2O_3-supported sample is most probably attributable to the formation of a spinel $CoAl_2O_4$ phase or other inactive surface species involving intimate contact between highly dispersed Co and surface Al_2O_3 sites [21,24] as indicated in the discussion of the TPR profiles.

Previously a correlation between the ease of catalyst reducibility and methane combustion activity has been proposed with oxides reduced at a lower temperature giving rise to a mechanism with a lower activation energy [11]. A similar correlation exists in the current study for supported oxides with alumina-supported samples which required particularly high-temperatures of reduction in TPR experiments (see Fig. 6) showing poorest performance in catalytic activity tests (see Table 2).

From Table 2, it can be seen that for supported cobalt oxide catalysts, exposure to the stoichiometric air–methane reaction mixture during Run 1 generally resulted in decreased light-off activity during subsequent testing in Run 2. As discussed above, this was also the case for the unsupported cobalt oxides with possible explanations for the deactivation including sintering of the active phase during testing or conversion of an active Co_3O_4 phase to less active CoO when exposed to temperatures above 450°C [11]. A 5 wt.% Co/ZrO_2 catalyst calcined at the higher temperature of 600°C was considerably less active than a corresponding sample calcined at 400°C which again is probably associated with such sintering or phase conversion phenomena causing decreased activity after exposure to the higher temperature. This shows that, even in the

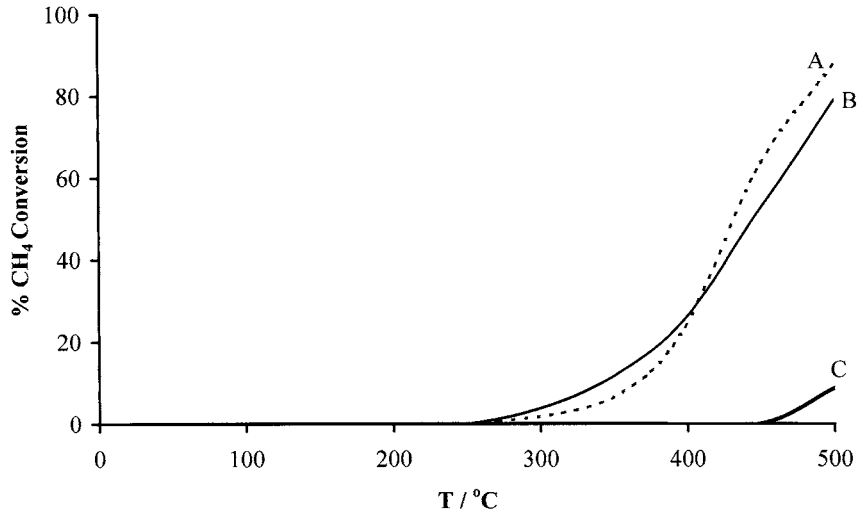

Fig. 10. CH_4 conversion as a function of temperature for supported Co (15 wt.%) catalysts: (A) Co/ZrO_2; (B) Co/CeO_2; and (C) Co/Al_2O_3.

absence of alumina, the possibility of catalyst deactivation during operation must be considered if cobalt oxide is to become a viable commercial alternative to, or additive in, noble metal combustion catalysts. The potential of employing higher surface area CeO_2 and ZrO_2 materials will be investigated in a further study.

4. Conclusions

SIP-MS was used to determine the effects of different support materials on the thermal decomposition of cobalt nitrate hexahydrate under linear heating rate conditions. Compared to the unsupported nitrate, completion of the decomposition process was delayed until higher temperatures for all the supported samples analysed. In particular, dispersion of $Co(NO_3)_2{\cdot}6H_2O$ on Al_2O_3 had a pronounced effect on the decomposition profile observed while ZrO_2 and CeO_2 supports resulted in more subtle changes to the decomposition profile. This was attributed to strong interactions between cobalt ions and the high surface area Al_2O_3–support material during preparation. TPR–MS profiles also indicated the presence of an intimate metal–support interaction upon calcination of Al_2O_3-supported cobalt nitrate in air which had a strong detrimental effect on the activity for methane combustion. For CeO_2 and ZrO_2 supported samples, TPR profiles were consistent with a two step reduction of Co_3O_4 via CoO to metal. Cobalt oxide supported on ceria or zirconia was shown to be a highly active catalyst for the combustion of CH_4, although in both cases, deactivation was observed upon exposure to the reaction mixture which may be associated with sintering or the conversion of Co_3O_4 to a less active CoO phase. Experiments to determine the extent of this deactivation over longer periods of exposure are now underway.

References

[1] D.L. Trimm, Appl. Catal. 7 (1983) 249.
[2] M.F.M. Zwinkels, S.G. Jaras, P.G. Menon, Catal. Rev. Sci. Eng. 35 (1993) 319.
[3] J.T. Kummer, Progr. Energy Combust. Sci. 6 (1980) 177.
[4] V.R. Choudray, B.S. Uphade, S.G. Pataskar, A. Keshavaraja, Angew. Chem. Int. Ed. Eng. 35 (1996) 2393.
[5] L.A. Isupova, G.M. Alikina, O.I. Snegurenko, V.A. Sadykov, S.V. Tsbulya, Appl. Catal. B 21 (1999) 171.
[6] R.J.H. Grisel, P.J. Kooyman, B.E. Nieuwenhuys, J. Catal. 191 (2000) 430.
[7] R.B. Anderson, K.C. Stein, J.J. Feenan, L.J.E. Hofer, Ind. Eng. Chem. 53 (1961) 809.
[8] W.P. Yant, C.O. Hawk, J. Am. Chem. Soc. 49 (1927) 1454.
[9] P.Y. Lin, M. Skoglundh, L. Lowendahl, J.E. Otterstedt, L. Dahl, K. Jansson ans, M. Nygren, Appl. Catal. B 6 (1995) 237.
[10] A. Törncrona, M. Skoglundh, P. Thormählen, E. Fridell, E. Jobson, Appl. Catal. B 14 (1997) 131.
[11] S. Arnone, G. Bagnasco, G. Busca, L. Lisi, G. Russo, M. Turco, in: A. Parmaliana, D. Sanfilippo, F. Frusteri, A. Vaccari, F. Arena (Eds.), Natural Gas Conversion V, Studies in Surface Science and Catalysis, Vol. 119, Elsevier, Amsterdam, 1998, p. 65.
[12] M. Skoglundh, A. Torncrona, P. Tormahlen, E. Fridell, A. Drewsen and E. Jobson, in: N. Kruse, A. Frennet, J.-M. Bastin (Eds.), Catalysis and Automotive Pollution Control IV, Studies in Surface Science and Catalysis, Vol. 116, Elsevier, Amsterdam, 1998, p. 113.
[13] M. Niwa, K. Awano, Y. Murakami, Appl. Catal. 7 (1983) 317.
[14] Y.M. Yang, B.Z. Wan, Appl. Catal. A 114 (1994) 35.
[15] M.J. Tiernan, P.A. Barnes, G.M.B. Parkes, J. Phys. Chem. B 103 (1999) 6944.
[16] N.W. Hurst, S.J. Gentry, A. Jones, B.D.Mc. Nicol, Catal. Rev. Sci. Eng. 24 (1982) 233.
[17] M.J. Tiernan, P.A. Barnes, G.M.B. Parkes, J. Phys. Chem. B 103 (1999) 338.
[18] T. Cseri, S. Békássy, G. Kenessey, G. Liptay, F. Figueras, Thermochim. Acta 288 (1996) 137.
[19] S.A.A. Mansour, Mater. Chem. Phys. 36 (1994) 317.
[20] P.A. Barnes, M.J. Tiernan, G.M.B. Parkes, J. Therm. Anal. Calorim. 56 (1999) 733.
[21] P.G. Dimitroa, D.R. Mehandjiev, J. Catal. 145 (1994) 356.
[22] P. Arnoldy, J.A. Moulijn, J. Catal. 93 (1985) 38.
[23] H.-C. Tung, C.-H. Yeh, J. Catal. 122 (1990) 211.
[24] R. Bechera, D. Balloy, J.Y. Dauphin, J. Grimblot Chem. Mater. 11 (1999) 1703.
[25] J.M. Criado, A. Ortega, F. Gotor, Thermochim. Acta 157 (1990) 171.
[26] M.E. Brown, M. Maciejewski, S. Vyazovkin, R. Komen, J. Sempere, A. Burnham, J. Opfermann, R. Strey, H.L. Anderson, A. Kemmler, R. Keuleers, J. Janssens, H.O. Desseyn, C.-R. Li, B. Boduit, J. Malek, T. Mitsuhashi, Thermochim. Acta 355 (2000) 125.
[27] V.D. Sokolovskii, Catal. Rev. Sci. Eng. 32 (1990) 1.
[28] E. Finocchio, G. Busca, V. Lerenzelli, V.S. Escribano, J. Chem. Soc. Faraday Trans. 92 (1996) 1587.
[29] C.F. Cullis, B.M. Willatt, J. Catal. 83 (1983) 267.
[30] S.H. Oh, P.J. Mitchell, R.M. Siewert, J. Catal. 132 (1991) 287.
[31] R.F. Hicks, H. Qi, M.L. Young, R.G. Lee, J. Catal. 122 (1990) 280.
[32] F. Zamar, A. Trovarelli, C. de Leitenburg, G. Dolcetti, J. Chem. Soc. Chem. Commun. 9 (1995) 965.